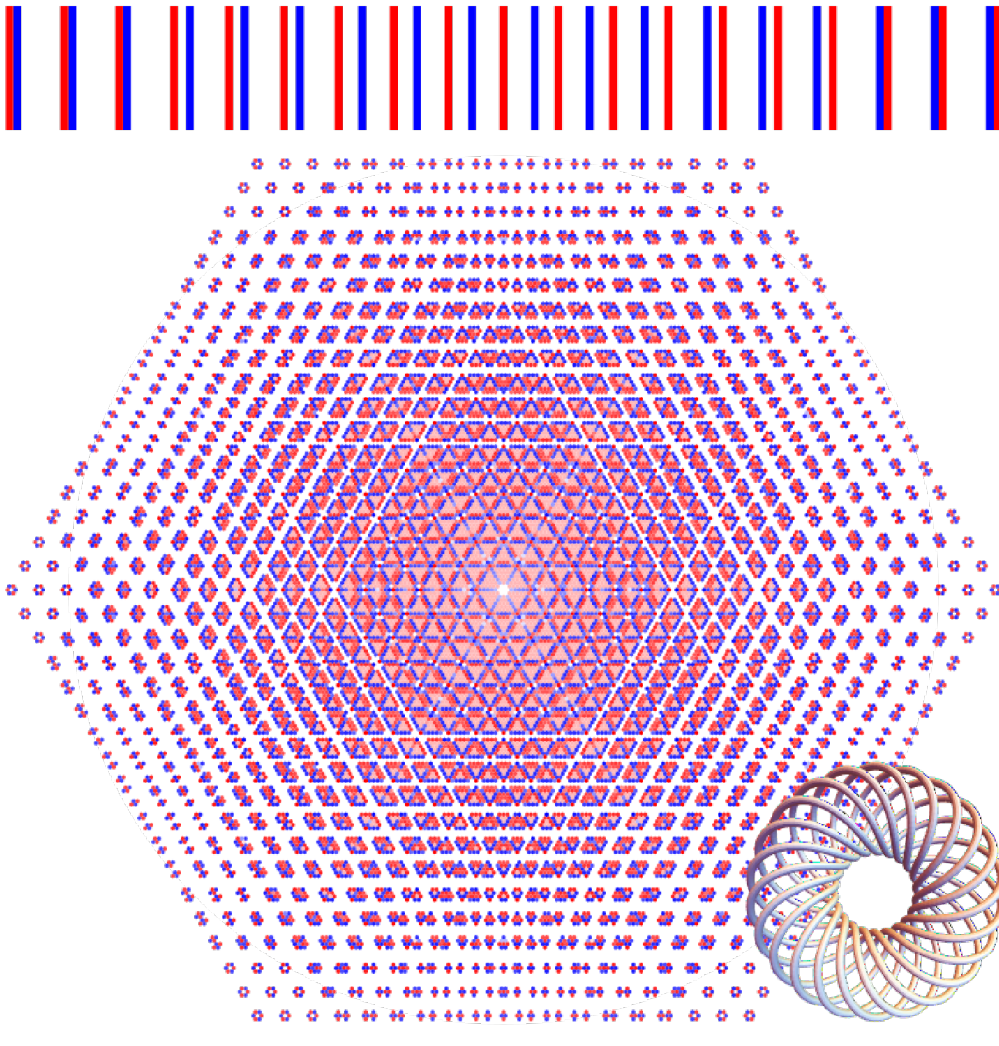
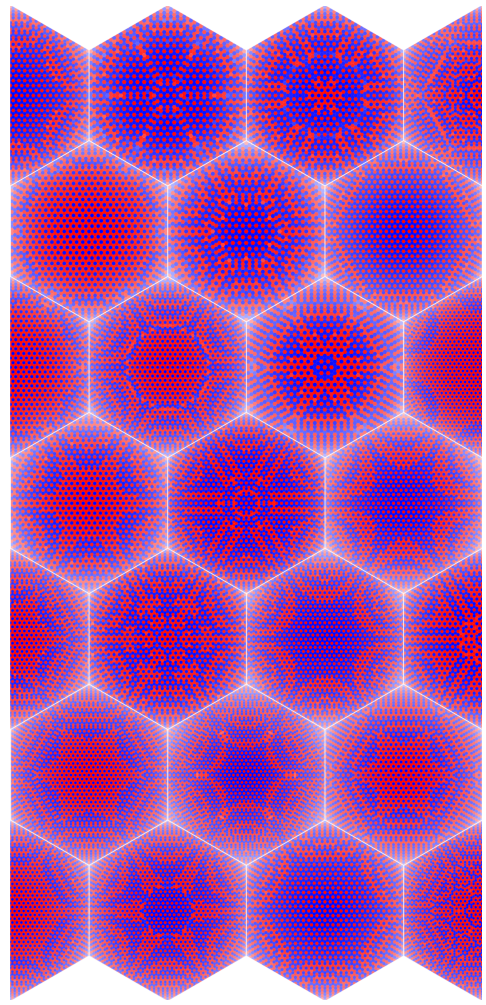


The 132-crossing torus knot $T_{22/7}$:



(many more at [ωβ/TK](#))

Random knots from [DHOEBL] with 51 – 75 crossings: (many more at [ωβ/DK](#))



Moral. We must come to terms with Θ !

Task 1. Make the “data” formulas human friendly.

Task 2. Prove the hexagonal symmetry of $\theta(K)$, and that $\theta(K) = \theta(-K) = -\theta(\bar{K})$.

That's harder than it seems! The formulas don't naively show any of that. Δ has a palindromic symmetry first conjectured in Alexander's original paper [Al] — it is invariant under $T \rightarrow T^{-1}$. Proving this took a few years, and the proof starting from the Wirtinger presentation is quite involved (e.g. [CF, Chapter IX]).

Task 3. Show that θ dominates the Rozansky-Overbay invariant ρ_1 [Ro1, Ro2, Ro4, Ov, BV1]. Precisely, show that $\rho_1 = -\theta|_{T_1 \rightarrow T, T_2 \rightarrow 1}$.

This one should be easy with techniques from [BV3, Section 4.2].

Task 4. Explain the “Chladni patterns”. Are there “dominant parts” of θ that can be computed in isolation?



left: © Whipple Museum of the History of Science, University of Cambridge; right: CC-BY-SA 4.0 / Wikimedia / Matemateca (IME USP) / Rodrigo Tetsuo Argenton

Task 5. Prove the genus bound of Conjecture 1.

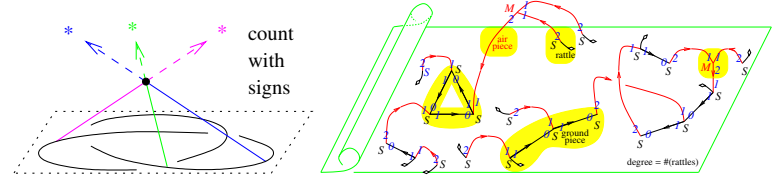
This is probably coming. One can bound the degree of $\Delta = \det(A)$ in terms of $g(K)$ using the Seifert presentation of the Alexander module. Pushing further, likely one can bound the degree of

$(g_{\alpha\beta}) = A^{-1}$ in terms of $g(K)$, and that's probably enough.

Task 6. Find a 3D interpretation of the $g_{\alpha\beta}$'s.

They must be closely related to the equivariant linking numbers of [KY, GK, GT, Oh3, Le1].

Task 7. Find a formula \mathcal{F} for $\Theta(K)$ that starts from a Seifert surface Σ of K . Better if \mathcal{F} is completely 3D! Assuming Task 13, it is known that Θ depends only of invariants of type ≤ 3 of Σ . Maybe \mathcal{F} is about configuration space integrals / chopstick towers? See CS: [Th, Le2, BN1], BF: [CR, BN2]



Task 8. Is there an intrinsic theory of finite type invariants for Seifert surfaces? For task 11, does its gr map to functions on H_1 ?

My current best understanding of finite type invariants for Seifert surfaces goes through thick graphs.



Task 9. Prove the the fibered condition of Conjecture 2.

If K is fibered, $\deg \Delta(K) = g(K)$ and $\Delta(K)$ is monic. Indeed, K is then the mapping cylinder of a diffeomorphism $f: \Sigma \rightarrow \Sigma$. The Alexander module of K is generated by $H_1(\Sigma)$ with relations

$\{\gamma = Tf_*\gamma: \gamma \in H_1(\Sigma)\}$. Thus the highest monomial in Δ is $T^g \det(f_*)$ and $\det(f_*) = \pm 1$ as f_* preserves the intersection pairing. If only we had a formula for θ in terms of f ...

Task 10. In general, find a formula for Θ corresponding to each known presentation of the Alexander module.

Wirtinger is $2\{\text{xings}\} \rightarrow \{\text{edges}\}$. Dehn is $\{\text{xings}\} \rightarrow \{\text{faces}\}$. Co-Dehn is $\{\text{faces}\} \rightarrow \{\text{xings}\}$. Burau is $\{\text{braid strands}\} \rightarrow \{\text{braid strands}\}$. Seifert is $H_1(\Sigma) \rightarrow H_1(\Sigma)$, and so is the presentation from Task 9. Grid diagrams lead to $\{\text{grid number}\} \rightarrow \{\text{grid number}\}$ (may relate to HFK). There's more!

Task 11. Write up the integration story.

Claim (e.g., [BN4]). Cutting corners, with $\epsilon^2 = 0$,

$$\frac{1}{\Delta_1 \Delta_2 \Delta_3} \exp\left(\epsilon \cdot \frac{\theta}{\Delta_1 \Delta_2 \Delta_3}\right) \sim \oint_{\prod_e \mathbb{R}_{p_{1e}, p_{2e}, p_{3e}, x_{1e}, x_{2e}, x_{3e}}^6} \prod_c \mathbb{E}^{L_c},$$

where \oint denotes perturbed formal Gaussian integration (i.e., “Feynman Diagrams”) and L_c is

$$\begin{aligned} L[X_{i,j} [S]] := & \text{Plus} [\\ & \sum_{v=1}^3 (x_{vi} (p_{vi^+} - p_{vi}) + x_{vj} (p_{vj^+} - p_{vj}) + (T_v^S - 1) x_{vi} (p_{vi^+} - p_{vj^+})), \\ & (T_v^S - 1) p_{3j} x_{1i} (T_v^S x_{2i} - x_{2j}), \\ & \epsilon S (T_v^S - 1) p_{1j} (p_{2i} - p_{2j}) x_{3i} / (T_v^S - 1), \\ & \epsilon S (1/2 + T_2^S p_{1i} p_{2j} x_{1i} x_{2i} - p_{1i} p_{2j} x_{1i} x_{2j} - p_{3i} x_{3i} - (T_2^S - 1) p_{2j} p_{3i} x_{2i} x_{3i} + \\ & (T_3^S - 1) p_{2j} p_{3j} x_{2i} x_{3j} + 2 p_{2j} p_{3i} x_{2j} x_{3i} + p_{1i} p_{3j} x_{1i} x_{3j} - p_{2i} p_{3j} x_{2i} x_{3j} - \\ & T_2^S p_{2j} p_{3j} x_{2i} x_{3j} + \\ & ((T_1^S - 1) p_{1j} x_{1i} (T_2^S p_{2i} x_{2i} - T_2^S p_{2j} x_{2j} - (T_2^S + 1) (T_3^S - 1) p_{3j} x_{3i} + \\ & T_2^S p_{3j} x_{3j}) + (T_3^S - 1) p_{3j} x_{3i} + \\ & (1 - T_2^S p_{1i} x_{1i} + p_{2i} x_{2j} + (T_2^S - 2) p_{2j} x_{2j}) / (T_2^S - 1))] \end{aligned}$$

In fact, we first found L_c using the method of undetermined coefficients, and then derived F_1 and F_2 from it.

Task 12. Find a similar perturbed Gaussian integral formula for θ , but with integration over $6H_1(\Sigma)$. The quadratic Q will be the same as in the Seifert-Alexander formula (but repeated 3 times, for each T_v). The perturbation P_ϵ will be given by low-degree finite type invariants of curves on Σ (possibly also dependent on the intersection points of such curves, or on other information coming from Σ).

Task 13. Prove that θ is equal to the two-loop contribution $Z^{(2)}$ to the Kontsevich integral Z .

Composed with the inverse PBW isomorphism $\chi^{-1}, \chi^{-1} \circ Z$ takes values in unitivalent Jacobi diagrams, $\mathcal{B} = \{\text{---}\circ\text{---}\dots\}/\text{IHX}$. Rozansky conjectured [Ro3, GR] and Kricker proved [Kr] that

$$\log(\chi^{-1} \circ Z) = f_1 \begin{array}{c} t \\ \square \end{array} + f_2 \begin{array}{c} t_1 \\ \square \\ t_2 \end{array} + \text{higher loops},$$

where $t^k \begin{array}{c} t \\ \square \end{array} := \begin{array}{|c|c|c|c|} \hline & & \cdots & n \cdots & | \\ \hline \end{array}$, $f_1 \in \mathbb{Q}[[t]]$, and $f_2 \in \mathbb{Q}[[t_1, t_2]]$ satisfy $f_1 = \frac{1}{2} \log \frac{\sinh(t/2)}{t \Delta(e^t)/2}$ and $f_2 = Z^{(2)}(\mathbb{E}^{t_1}, \mathbb{E}^{t_2}) / \Delta(\mathbb{E}^{t_1}) \Delta(\mathbb{E}^{t_1}) \Delta(\mathbb{E}^{t_1+t_2})$ where $Z^{(2)} \in \mathbb{Z}[T_1^{\pm 1}, T_2^{\pm 1}]$ is the “two loop polynomial”. Ohtsuki [Oh2] studied $Z^{(2)}$ extensively, and almost certainly, $Z^{(2)} = \theta$. Prove that!

Task 14. Complete and write up the \mathfrak{g}_ϵ^+ story.

Let \mathfrak{g} be a semisimple Lie algebra, let \mathfrak{h} be its Cartan subalgebra, and let \mathfrak{b}^u and \mathfrak{b}^l be its upper and lower Borel subalgebras. Then \mathfrak{b}^u has a bracket β , and as the dual of \mathfrak{b}^l it also has a cobracket δ , and in fact, $\mathfrak{g} \oplus \mathfrak{h} \equiv \text{Double}(\mathfrak{b}^u, \beta, \delta)$. Let $\mathfrak{g}_\epsilon^+ := \text{Double}(\mathfrak{b}^u, \beta, \epsilon \delta)$ (mod ϵ^{d+1} it is solvable for any d). We expect that Θ is the universal invariant (in the sense of Lawrence and Ohtsuki [La, Oh1]) corresponding to $sl_{3,\epsilon}^+$, computed modulo ϵ^2 (in fact, that's how we guessed it). See [BN3, BV2].

Task 15. Go beyond sl_3 and the first power of ϵ !

This sounds very appealing, and you will indeed get stronger and stronger invariants. But they will become less and less computable \odot .

Task 16. Relate the \mathfrak{g}_ϵ^+ story with (rotational) virtual knots [Kau], with $\vec{\mathcal{A}}$ [Po], and with quantization of Lie bialgebras [EK1, EK2, En, Se]

we expect that
There is a
commutative
diagram as
Re top on
on the right
which descends to
The bottom one,
with \oplus Re
case of $\mathfrak{g} = sl_3$
 \oplus \mathfrak{h}
But \oplus
 \oplus

Task 17. Find a w -style characterization of Θ .

A word about [GR].

Compare with (say) [BD], where Δ is characterized on w -knots by the overcrossings / tails commute relation. Similarly, it should be possible to characterize Θ on rotational virtual knots by some “overcrossings / tails nearly commute” relation.

Task 18. Understand Chern-Simons theory with gauge group \mathfrak{g}_ϵ^+ .

Is there a gauge that leads to the formula \mathcal{F} of Task 7?

Task 19. What happens to representation theory as $\epsilon \rightarrow 0$? Is there any fun in continuous morphisms $\mathfrak{g}_\epsilon^+ \rightarrow \mathfrak{gl}_{n,\epsilon}^+$?

Task 20. Does Θ extend to knots in $\mathbb{Z}\text{HS}/\mathbb{Q}\text{HS}$?

Z and $Z^{(2)}$ do.

Task 21. Is there a surgery formula for Θ ?

Z and $Z^{(2)}$ have.

Task 22. Extend Θ to tangles and figure out how it behaves under strand doubling.

Z and $Z^{(2)}$ extend but their extensions depend on parenthesizations. From Task 14 we expect that Θ will extend without the need for parenthesizations, yet with an asymmetry built into the doubling operations. 

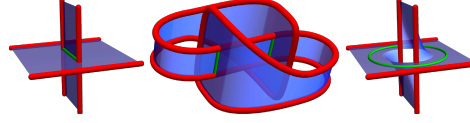
Task 23. Make Kricker/Ohtsuki [Kr, Oh2] more computable!

Task 24. Find a multi-variable version of θ for links, like there is a multi-variable Alexander for links (e.g. [Kaw, Chapter 7]).

It is predicted g_e^+ consideration, but not by the loop expansion.

Task 25. Find a ribbon condition satisfied by Θ .

For a ribbon knot K , one may find a Seifert surface Σ half of whose homology is generated by the components of an unlink embedded in Σ . This makes for a presentation matrix A of the Alexander module of K that has big blocks of zeros, and this leads to the Fox-Milnor condition [FM], $\Delta \doteq \det(A) \doteq f(T)f(T^{-1})$ for some $f \in \mathbb{Z}[T^{\pm 1}]$. If $\det A$ is constrained for ribbon knots, perhaps so is A^{-1} and therefore Θ ?



Bonus Task. Carthago delenda est and every knot polynomial must be categorified.

M. Khovanov & Cato the Elder



[Al] J. W. Alexander, *Topological invariants of knots and links*, Trans. Amer. Math. Soc. **30** (1928) 275–306.

[BN1] D. Bar-Natan, *Cosmic Coincidences and Several Other Stories*, talk given in Tennessee, March 2011. Handout and video: oef/Ten.

[BN2] D. Bar-Natan, *A Partial Reduction of BF Theory to Combinatorics*, talk given in Vienna, February 2014. Handout and video: oef/Vie.

References.

[BN3] D. Bar-Natan, *Everything around sl_2^c is DoPeGDO. So what?*, talk given in “Quantum Topology and Hyperbolic Geometry Conference”, Da Nang, Vietnam, May 2019. Handout and video at oef/DPG.

[BN4] D. Bar-Natan, *Knot Invariants from Zero-Dimensional QFT*, talk given in Bonn, May 2025. Handout and video: oef/Bonn.

[BD] D. Bar-Natan and Z. Dancso, *Finite Type Invariants of W-Knotted Objects I: W-Knots and the Alexander Polynomial*, Alg. and Geom. Top. **16-2** (2016) 1063–1133, [arXiv:1405.1956](https://arxiv.org/abs/1405.1956).

[BV1] D. Bar-Natan and R. van der Veen, *A Perturbed-Alexander Invariant*, Quantum Topology **15** (2024) 449–472, [arXiv:2206.12298](https://arxiv.org/abs/2206.12298).

[BV2] D. Bar-Natan and R. van der Veen, *Perturbed Gaussian Generating Functions for Universal Knot Invariants*, [arXiv:2109.02057](https://arxiv.org/abs/2109.02057).

[BV3] D. Bar-Natan and R. van der Veen, *A Fast, Strong, Topologically Meaningful, and Fun Knot Invariant*, [oef/Theta](https://arxiv.org/abs/2509.18456) and [arXiv:2509.18456](https://arxiv.org/abs/2509.18456).

[CR] A. S. Cattaneo and C. A. Rossi, *Wilson Surfaces and Higher Dimensional Knot Invariants*, Comm. Math. Phys. **256** (2005) 513–537, [arXiv:math/0210037](https://arxiv.org/abs/math/0210037).

[CF] R. H. Crowell and R. H. Fox, *Introduction to Knot Theory*, Springer-Verlag GTM **57** (1963).

[DHOEFL] N. Dunfield, A. Hirani, M. Obeidin, A. Ehrenborg, S. Bhattacharya, D. Lei, and others, *Random Knots: A Preliminary Report*, lecture notes at oef/DHOEFL. Also a data file at oef/DD.

[En] B. Enriquez, *A Cohomological Construction of Quantization Functors of Lie Bialgebras*, Adv. in Math. **197-2** (2005) 430–479, [arXiv:math/0212325](https://arxiv.org/abs/math/0212325).

[EK1] P. Etingof and D. Kazhdan, *Quantization of Lie Bialgebras, I*, Sel. Math., NS **2** (1996) 1–41, [arXiv:q-alg/9506005](https://arxiv.org/abs/q-alg/9506005).

[EK2] P. Etingof and D. Kazhdan, *Quantization of Lie bialgebras, II*, Sel. Math., NS **4** (1998) 213–231, [arXiv:q-alg/9701038](https://arxiv.org/abs/q-alg/9701038).

[FM] R. H. Fox and J. W. Milnor, *Singularities of 2-Spheres in 4-Space and Cobordism of Knots*, Osaka J. Math. **3-2** (1966) 257–267.

[GK] S. Garoufalidis and A. Kricker, *A Rational Noncommutative Invariant of Boundary Links*, Geom. & Top. **8** (2004) 115–204, [arXiv:math/0105028](https://arxiv.org/abs/math/0105028).

[GR] S. Garoufalidis and L. Rozansky, *The Loop Expansion of the Kontsevich Integral, the Null-Move, and S-Equivalence*, [arXiv:math/0003187](https://arxiv.org/abs/math/0003187).

[GT] S. Garoufalidis and P. Teichner, *On Knots with Trivial Alexander Polynomial*, J. Diff. Geom. **67** (2004) 165–191, [arXiv:math/0206023](https://arxiv.org/abs/math/0206023).

[Kau] L. H. Kauffman, *Rotational Virtual Knots and Quantum Link Invariants*, J. of Knot Theory and its Ramifications **24-13** (2015), [arXiv:1509.00578](https://arxiv.org/abs/1509.00578).

[Kaw] A. Kawauchi, *A Survey of Knot Theory*, Birkhauser Verlag, 1996.

[KY] S. Kojima and M. Yamada, *Some New Invariants of Links*, Invent. Math. **54** (1979) 213–228.

[Kr] A. Kricker, *The Lines of the Kontsevich Integral and Rozansky’s Rationality Conjecture*, [arXiv:math/0005284](https://arxiv.org/abs/math/0005284).

[La] R. J. Lawrence, *Universal Link Invariants using Quantum Groups*, Proc. XVII Int. Conf. on Diff. Geom. Methods in Theor., Chester, England, August 1988. World Scientific (1989) 55–63.

[Le1] C. Lescop, *Knot Invariants Derived from the Equivariant Linking Pairing*, AMS/IP Stud. in Adv. Math. **50** (2011) 217–242, [arXiv:1001.4474](https://arxiv.org/abs/1001.4474).

[Le2] C. Lescop, *Invariants of Links and 3-Manifolds from Graph Configurations*, EMS Monographs, 2024, [arXiv:2001.09929](https://arxiv.org/abs/2001.09929).

[Oh1] T. Ohtsuki, *Quantum Invariants*, Series on Knots and Everything **29**, World Scientific 2002.

[Oh2] T. Ohtsuki, *On the 2-Loop Polynomial of Knots*, Geometry & Topology **11** (2007) 1357–1475.

[Oh3] T. Ohtsuki, *Invariants of Knots Derived from Equivariant Linking Matrices of their Surgery Presentations*, Int. J. Math. **20-7** (2009) 883–913.

[Ov] A. Overby, *Perturbative Expansion of the Colored Jones Polynomial*, Ph.D. thesis, University of North Carolina, August 2013, oef/Ov.

[Po] M. Polyak, *On the Algebra of Arrow Diagrams*, Let. Math. Phys. **51** (2000) 275–291.

[Ro1] L. Rozansky, *A Contribution of the Trivial Flat Connection to the Jones Polynomial and Witten’s Invariant of 3D Manifolds*, I. Comm. Math. Phys. **175-2** (1996) 275–296, [arXiv:hep-th/9401061](https://arxiv.org/abs/hep-th/9401061).

[Ro2] L. Rozansky, *The Universal R-Matrix, Burau Representation and the Melvin-Morton Expansion of the Colored Jones Polynomial*, Adv. Math. **134-1** (1998) 1–31, [arXiv:q-alg/9604005](https://arxiv.org/abs/q-alg/9604005).

[Ro3] L. Rozansky, *A Rational Structure of Generating Functions for Vassiliev Invariants*, Yale University preprint, July 1999.

[Ro4] L. Rozansky, *A Universal U(1)-RCC Invariant of Links and Rationality Conjecture*, [arXiv:math/0201139](https://arxiv.org/abs/math/0201139).

[Se] P. Ševera, *Quantization of Lie Bialgebras Revisited*, Sel. Math., NS, to appear, [arXiv:1401.6164](https://arxiv.org/abs/1401.6164).

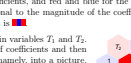
[Th] D. Thurston, *Integral expressions for the Vassiliev knot invariants*, Harvard University senior thesis, April 1995, [arXiv:math.QA/9901110](https://arxiv.org/abs/math.QA/9901110).

A: Note that ~~tangles & strand doubling~~ are keys to “Algebraic Knot Theory” [AKT].

letter if longer.

A FAST, STRONG, TOPOLOGICALLY MEANINGFUL, AND FUN KNOT INVARIANT

DROR BAR-NATAN AND ROLAND VAN DER VEEN

ABSTRACT. In this paper we discuss a pair of polynomial knot invariants $\Theta = (\Delta, \theta)$ which are nearly identical. The first, Δ , is old news, the Alexander polynomial [Al]. It is a special case of the 2-variable Laurent polynomial in variables T_1 and T_2 . The second, θ , is new. It is a 2-variable Laurent polynomial in variables T_1 and T_2 . We can turn such a polynomial into a 2D array of coefficients and then into a chain of bars of varying colors, while for the zero coefficients, and red and blue for the positive and negative coefficients (with intensity proportional to the magnitude of the coefficients). The result is a “QR code” and for the knot Θ it is 

Similarly, Θ is a 2-variable Laurent polynomial in variables T_1 and T_2 . We can turn such a polynomial into a 2D array of coefficients and then into a picture. To highlight a certain conjectured hexagonal symmetry of the resulting picture, we turn the picture into a hexagonal QR code. To highlight the polynomial $\Theta = T_1T_2 + T_1^{-1}T_2^{-1}$, we turn it into a 2D picture corresponding to the polynomial $2 + T_1T_2 + T_1^{-1}T_2^{-1} + T_1^{-1}T_2^{-1} = T_1^2$. Thus Θ is a “QR code” picture: a bar code with the knot (or knotoid) appended (at the start), they are in Figure 1.1. For some alternating square wave knots, like in Figure 1.2, and for a random square wave, in Figure 1.3. In addition, the hexagonal QR codes of 15 knots with > 300 crossings are in Figure 1.4, and Θ of a 132-crossing torus knot is in Figure 3.1. Some “Chladni figures” formed by powder atop vibrating plates (on right) are not present any more, but the QR codes are still there, and they are in Figure 1.1. For some alternating square wave knots, like in Figure 1.2, and for a random square wave, in Figure 1.3. In addition, the hexagonal QR codes of 15 knots with > 300 crossings are in Figure 1.4, and Θ of a 132-crossing torus knot is in Figure 3.1. Some “Chladni figures” formed by powder atop vibrating plates (on right) are not present any more, but the QR codes are still there, and they are in Figure 1.1. For some alternating square wave knots, like in Figure 1.2, and for a random square wave, in Figure 1.3. In addition, the hexagonal QR codes of 15 knots with > 300 crossings are in Figure 1.4, and Θ of a 132-crossing torus knot is in Figure 3.1. Some “Chladni figures” formed by powder atop vibrating plates (on right) are not present any more, but the QR codes are still there, and they are in Figure 1.1. For some alternating square wave knots, like in Figure 1.2, and for a random square wave, in Figure 1.3. In addition, the hexagonal QR codes of 15 knots with > 300 crossings are in Figure 1.4, and Θ of a 132-crossing torus knot is in Figure 3.1. Some “Chladni figures” formed by powder atop vibrating plates (on right) are not present any more, but the QR codes are still there, and they are in Figure 1.1. For some alternating square wave knots, like in Figure 1.2, and for a random square wave, in Figure 1.3. In addition, the hexagonal QR codes of 15 knots with > 300 crossings are in Figure 1.4, and Θ of a 132-crossing torus knot is in Figure 3.1. Some “Chladni figures” formed by powder atop vibrating plates (on right) are not present any more, but the QR codes are still there, and they are in Figure 1.1. For some alternating square wave knots, like in Figure 1.2, and for a random square wave, in Figure 1.3. In addition, the hexagonal QR codes of 15 knots with > 300 crossings are in Figure 1.4, and Θ of a 132-crossing torus knot is in Figure 3.1. Some “Chladni figures” formed by powder atop vibrating plates (on right) are not present any more, but the QR codes are still there, and they are in Figure 1.1. For some alternating square wave knots, like in Figure 1.2, and for a random square wave, in Figure 1.3. In addition, the hexagonal QR codes of 15 knots with > 300 crossings are in Figure 1.4, and Θ of a 132-crossing torus knot is in Figure 3.1. Some “Chladni figures” formed by powder atop vibrating plates (on right) are not present any more, but the QR codes are still there, and they are in Figure 1.1. For some alternating square wave knots, like in Figure 1.2, and for a random square wave, in Figure 1.3. In addition, the hexagonal QR codes of 15 knots with > 300 crossings are in Figure 1.4, and Θ of a 132-crossing torus knot is in Figure 3.1. Some “Chladni figures” formed by powder atop vibrating plates (on right) are not present any more, but the QR codes are still there, and they are in Figure 1.1. For some alternating square wave knots, like in Figure 1.2, and for a random square wave, in Figure 1.3. In addition, the hexagonal QR codes of 15 knots with > 300 crossings are in Figure 1.4, and Θ of a 132-crossing torus knot is in Figure 3.1. Some “Chladni figures” formed by powder atop vibrating plates (on right) are not present any more, but the QR codes are still there, and they are in Figure 1.1. For some alternating square wave knots, like in Figure 1.2, and for a random square wave, in Figure 1.3. In addition, the hexagonal QR codes of 15 knots with > 300 crossings are in Figure 1.4, and Θ of a 132-crossing torus knot is in Figure 3.1. Some “Chladni figures” formed by powder atop vibrating plates (on right) are not present any more, but the QR codes are still there, and they are in Figure 1.1. For some alternating square wave knots, like in Figure 1.2, and for a random square wave, in Figure 1.3. In addition, the hexagonal QR codes of 15 knots with > 300 crossings are in Figure 1.4, and Θ of a 132-crossing torus knot is in Figure 3.1. Some “Chladni figures” formed by powder atop vibrating plates (on right) are not present any more, but the QR codes are still there, and they are in Figure 1.1. For some alternating square wave knots, like in Figure 1.2, and for a random square wave, in Figure 1.3. In addition, the hexagonal QR codes of 15 knots with > 300 crossings are in Figure 1.4, and Θ of a 132-crossing torus knot is in Figure 3.1. Some “Chladni figures” formed by powder atop vibrating plates (on right) are not present any more, but the QR codes are still there, and they are in Figure 1.1. For some alternating square wave knots, like in Figure 1.2, and for a random square wave, in Figure 1.3. In addition, the hexagonal QR codes of 15 knots with > 300 crossings are in Figure 1.4, and Θ of a 132-crossing torus knot is in Figure 3.1. Some “Chladni figures” formed by powder atop vibrating plates (on right) are not present any more, but the QR codes are still there, and they are in Figure 1.1. For some alternating square wave knots, like in Figure 1.2, and for a random square wave, in Figure 1.3. In addition, the hexagonal QR codes of 15 knots with > 300 crossings are in Figure 1.4, and Θ of a 132-crossing torus knot is in Figure 3.1. Some “Chladni figures” formed by powder atop vibrating plates (on right) are not present any more, but the QR codes are still there, and they are in Figure 1.1. For some alternating square wave knots, like in Figure 1.2, and for a random square wave, in Figure 1.3. In addition, the hexagonal QR codes of 15 knots with > 300 crossings are in Figure 1.4, and Θ of a 132-crossing torus knot is in Figure 3.1. Some “Chladni figures” formed by powder atop vibrating plates (on right) are not present any more, but the QR codes are still there, and they are in Figure 1.1. For some alternating square wave knots, like in Figure 1.2, and for a random square wave, in Figure 1.3. In addition, the hexagonal QR codes of 15 knots with > 300 crossings are in Figure 1.4, and Θ of a 132-crossing torus knot is in Figure 3.1. Some “Chladni figures” formed by powder atop vibrating plates (on right) are not present any more, but the QR codes are still there, and they are in Figure 1.1. For some alternating square wave knots, like in Figure 1.2, and for a random square wave, in Figure 1.3. In addition, the hexagonal QR codes of 15 knots with > 300 crossings are in Figure 1.4, and Θ of a 132-crossing torus knot is in Figure 3.1. Some “Chladni figures” formed by powder atop vibrating plates (on right) are not present any more, but the QR codes are still there, and they are in Figure 1.1. For some alternating square wave knots, like in Figure 1.2, and for a random square wave, in Figure 1.3. In addition, the hexagonal QR codes of 15 knots with > 300 crossings are in Figure 1.4, and Θ of a 132-crossing torus knot is in Figure 3.1. Some “Chladni figures” formed by powder atop vibrating plates (on right) are not present any more, but the QR codes are still there, and they are in Figure 1.1. For some alternating square wave knots, like in Figure 1.2, and for a random square wave, in Figure 1.3. In addition, the hexagonal QR codes of 15 knots with > 300 crossings are in Figure 1.4, and Θ of a 132-crossing torus knot is in Figure 3.1. Some “Chladni figures” formed by powder atop vibrating plates (on right) are not present any more, but the QR codes are still there, and they are in Figure 1.1. For some alternating square wave knots, like in Figure 1.2, and for a random square wave, in Figure 1.3. In addition, the hexagonal QR codes of 15 knots with > 300 crossings are in Figure 1.4, and Θ of a 132-crossing torus knot is in Figure 3.1. Some “Chladni figures” formed by powder atop vibrating plates (on right) are not present any more, but the QR codes are still there, and they are in Figure 1.1. For some alternating square wave knots, like in Figure 1.2, and for a random square wave, in Figure 1.3. In addition, the hexagonal QR codes of 15 knots with > 300 crossings are in Figure 1.4, and Θ of a 132-crossing torus knot is in Figure 3.1. Some “Chladni figures” formed by powder atop vibrating plates (on right) are not present any more, but the QR codes are still there, and they are in Figure 1.1. For some alternating square wave knots, like in Figure 1.2, and for a random square wave, in Figure 1.3. In addition, the hexagonal QR codes of 15 knots with > 300 crossings are in Figure 1.4, and Θ of a 132-crossing torus knot is in Figure 3.1. Some “Chladni figures” formed by powder atop vibrating plates (on right) are not present any more, but the QR codes are still there, and they are in Figure 1.1. For some alternating square wave knots, like in Figure 1.2, and for a random square wave, in Figure 1.3. In addition, the hexagonal QR codes of 15 knots with > 300 crossings are in Figure 1.4, and Θ of a 132-crossing torus knot is in Figure 3.1. Some “Chladni figures” formed by powder atop vibrating plates (on right) are not present any more, but the QR codes are still there, and they are in Figure 1.1. For some alternating square wave knots, like in Figure 1.2, and for a random square wave, in Figure 1.3. In addition, the hexagonal QR codes of 15 knots with > 300 crossings are in Figure 1.4, and Θ of a 132-crossing torus knot is in Figure 3.1. Some “Chladni figures” formed by powder atop vibrating plates (on right) are not present any more, but the QR codes are still there, and they are in Figure 1.1. For some alternating square wave knots, like in Figure 1.2, and for a random square wave, in Figure 1.3. In addition, the hexagonal QR codes of 15 knots with > 300 crossings are in Figure 1.4, and Θ of a 132-crossing torus knot is in Figure 3.1. Some “Chladni figures” formed by powder atop vibrating plates (on right) are not present any more, but the QR codes are still there, and they are in Figure 1.1. For some alternating square wave knots, like in Figure 1.2, and for a random square wave, in Figure 1.3. In addition, the hexagonal QR codes of 15 knots with > 300 crossings are in Figure 1.4, and Θ of a 132-crossing torus knot is in Figure 3.1. Some “Chladni figures” formed by powder atop vibrating plates (on right) are not present any more, but the QR codes are still there, and they are in Figure 1.1. For some alternating square wave knots, like in Figure 1.2, and for a random square wave, in Figure 1.3. In addition, the hexagonal QR codes of 15 knots with > 300 crossings are in Figure 1.4, and Θ of a 132-crossing torus knot is in Figure 3.1. Some “Chladni figures” formed by powder atop vibrating plates (on right) are not present any more, but the QR codes are still there, and they are in Figure 1.1. For some alternating square wave knots, like in Figure 1.2, and for a random square wave, in Figure 1.3. In addition, the hexagonal QR codes of 15 knots with > 300 crossings are in Figure 1.4, and Θ of a 132-crossing torus knot is in Figure 3.1. Some “Chladni figures” formed by powder atop vibrating plates (on right) are not present any more, but the QR codes are still there, and they are in Figure 1.1. For some alternating square wave knots, like in Figure 1.2, and for a random square wave, in Figure 1.3. In addition, the hexagonal QR codes of 15 knots with > 300 crossings are in Figure 1.4, and Θ of a 132-crossing torus knot is in Figure 3.1. Some “Chladni figures” formed by powder atop vibrating plates (on right) are not present any more, but the QR codes are still there, and they are in Figure 1.1. For some alternating square wave knots, like in Figure 1.2, and for a random square wave, in Figure 1.3. In addition, the hexagonal QR codes of 15 knots with > 300 crossings are in Figure 1.4, and Θ of a 132-crossing torus knot is in Figure 3.1. Some “Chladni figures” formed by powder atop vibrating plates (on right) are not present any more, but the QR codes are still there, and they are in Figure 1.1. For some alternating square wave knots, like in Figure 1.2, and for a random square wave, in Figure 1.3. In addition, the hexagonal QR codes of 15 knots with > 300 crossings are in Figure 1.4, and Θ of a 132-crossing torus knot is in Figure 3.1. Some “Chladni figures” formed by powder atop vibrating plates (on right) are not present any more, but the QR codes are still there, and they are in Figure 1.1. For some alternating square wave knots, like in Figure 1.2, and for a random square wave, in Figure 1.3. In addition, the hexagonal QR codes of 15 knots with > 300 crossings are in Figure 1.4, and Θ of a 132-crossing torus knot is in Figure 3.1. Some “Chladni figures” formed by powder atop vibrating plates (on right) are not present any more, but the QR codes are still there, and they are in Figure 1.1. For some alternating square wave knots, like in Figure 1.2, and for a random square wave, in Figure 1.3. In addition, the hexagonal QR codes of 15 knots with > 300 crossings are in Figure 1.4, and Θ of a 132-crossing torus knot is in Figure 3.1. Some “Chladni figures” formed by powder atop vibrating plates (on right) are not present any more, but the QR codes are still there, and they are in Figure 1.1. For some alternating square wave knots, like in Figure 1.2, and for a random square wave, in Figure 1.3. In addition, the hexagonal QR codes of 15 knots with > 300 crossings are in Figure 1.4, and Θ of a 132-crossing torus knot is in Figure 3.1. Some “Chladni figures” formed by powder atop vibrating plates (on right) are not present any more, but the QR codes are still there, and they are in Figure 1.1. For some alternating square wave knots, like in Figure 1.2, and for a random square wave, in Figure 1.3. In addition, the hexagonal QR codes of 15 knots with > 300 crossings are in Figure 1.4, and Θ of a 132-crossing torus knot is in Figure 3.1. Some “Chladni figures” formed by powder atop vibrating plates (on right) are not present any more, but the QR codes are still there, and they are in Figure 1.1. For some alternating square wave knots, like in Figure 1.2, and for a random square wave, in Figure 1.3. In addition, the hexagonal QR codes of 15 knots with > 300 crossings are in Figure 1.4, and Θ of a 132-crossing torus knot is in Figure 3.1. Some “Chladni figures” formed by powder atop vibrating plates (on right) are not present any more, but the QR codes are still there, and they are in Figure 1.1. For some alternating square wave knots, like in Figure 1.2, and for a random square wave, in Figure 1.3. In addition, the hexagonal QR codes of 15 knots with > 300 crossings are in Figure 1.4, and Θ of a 132-crossing torus knot is in Figure 3.1. Some “Chladni figures” formed by powder atop vibrating plates (on right) are not present any more, but the QR codes are still there, and they are in Figure 1.1. For some alternating square wave knots, like in Figure 1.2, and for a random square wave, in Figure 1.3. In addition, the hexagonal QR codes of 15 knots with > 300 crossings are in Figure 1.4, and Θ of a 132-crossing torus knot is in Figure 3.1. Some “Chladni figures” formed by powder atop vibrating plates (on right) are not present any more, but the QR codes are still there, and they are in Figure 1.1. For some alternating square wave knots, like in Figure 1.2, and for a random square wave, in Figure 1.3. In addition, the hexagonal QR codes of 15 knots with > 300 crossings are in Figure 1.4, and Θ of a 132-crossing torus knot is in Figure 3.1. Some “Chladni figures” formed by powder atop vibrating plates (on right) are not present any more, but the QR codes are still there, and they are in Figure 1.1. For some alternating square wave knots, like in Figure 1.2, and for a random square wave, in Figure 1.3. In addition, the hexagonal QR codes of 15 knots with > 300 crossings are in Figure 1.4, and Θ of a 132-crossing torus knot is in Figure 3.1. Some “Chladni figures” formed by powder atop vibrating plates (on right) are not present any more, but the QR codes are still there, and they are in Figure 1.1. For some alternating square wave knots, like in Figure 1.2, and for a random square wave, in Figure 1.3. In addition, the hexagonal QR codes of 15 knots with > 300 crossings are in Figure 1.4, and Θ of a 132-crossing torus knot is in Figure 3.1. Some “Chladni figures” formed by powder atop vibrating plates (on right) are not present any more, but the QR codes are still there, and they are in Figure 1.1. For some alternating square wave knots, like in Figure 1.2, and for a random square wave, in Figure 1.3. In addition, the hexagonal QR codes of 15 knots with > 300 crossings are in Figure 1.4, and Θ of a 132-crossing torus knot is in Figure 3.1. Some “Chladni figures” formed by powder atop vibrating plates (on right) are not present any more, but the QR codes are still there, and they are in Figure 1.1. For some alternating square wave knots, like in Figure 1.2, and for a random square wave, in Figure 1.3. In addition, the hexagonal QR codes of 15 knots with > 300 crossings are in Figure 1.4, and Θ of a 132-crossing torus knot is in Figure 3.1. Some “Chladni figures” formed by powder atop vibrating plates (on right) are not present any more, but the QR codes are still there, and they are in Figure 1.1. For some alternating square wave knots, like in Figure 1.2, and for a random square wave, in Figure 1.3. In addition, the hexagonal QR codes of 15 knots with > 300 crossings are in Figure 1.4, and Θ of a 132-crossing torus knot is in Figure 3.1. Some “Chladni figures” formed by powder atop vibrating plates (on right) are not present any more, but the QR codes are still there, and they are in Figure 1.1. For some alternating square wave knots, like in Figure 1.2, and for a random square wave, in Figure 1.3. In addition, the hexagonal QR codes of 15 knots with > 300 crossings are in Figure 1.4, and Θ of a 132-crossing torus knot is in Figure 3.1. Some “Chladni figures” formed by powder atop vibrating plates (on right) are not present any more, but the QR codes are still there, and they are in Figure 1.1. For some alternating square wave knots, like in Figure 1.2, and for a random square wave, in Figure 1.3. In addition, the hexagonal QR codes of 15 knots with > 300 crossings are in Figure 1.4, and Θ of a 132-crossing torus knot is in Figure 3.1. Some “Chladni figures” formed by powder atop vibrating plates (on right) are not present any more, but the QR codes are still there, and they are in Figure 1.1. For some alternating square wave knots, like in Figure 1.2, and for a random square wave, in Figure 1.3. In addition, the hexagonal QR codes of 15 knots with > 300 crossings are in Figure 1.4, and Θ of a 132-crossing torus knot is in Figure 3.1. Some “Chladni figures” formed by powder atop vibrating plates (on right) are not present any more, but the QR codes are still there, and they are in Figure 1.1. For some alternating square wave knots, like in Figure 1.2, and for a random square wave, in Figure 1.3. In addition, the hexagonal QR codes of 15 knots with > 300 crossings are in Figure 1.4, and Θ of a 132-crossing torus knot is in Figure 3.1. Some “Chladni figures” formed by powder atop vibrating plates (on right) are not present any more, but the QR codes are still there, and they are in Figure 1.1. For some alternating square wave knots, like in Figure 1.2, and for a random square wave, in Figure 1.3. In addition, the hexagonal QR codes of 15 knots with > 300 crossings are in Figure 1.4, and Θ of a 132-crossing torus knot is in Figure 3.1. Some “Chladni figures” formed by powder atop vibrating plates (on right) are not present any more, but the QR codes are still there, and they are in Figure 1.1. For some alternating square wave knots, like in Figure 1.2, and for a random square wave, in Figure 1.3. In addition, the hexagonal QR codes of 15 knots with > 300 crossings are in Figure 1.4, and Θ of a 132-crossing torus knot is in Figure 3.1. Some “Chladni figures” formed by powder atop vibrating plates (on right) are not present any more, but the QR codes are still there, and they are in Figure 1.1. For some alternating square wave knots, like in Figure 1.2, and for a random square wave, in Figure 1.3. In addition,

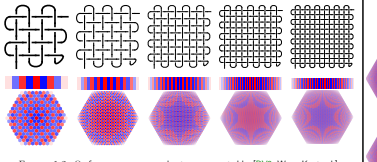


FIGURE 1.2. Θ of some square weave knots, as computed by [BV3, WeaveKnots.nb].

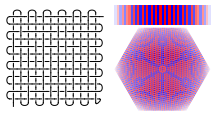


FIGURE 1.3. Θ of a randomized weave knot, as computed by [BV3, WeaveKnots.nb]. Crossings will be positive or negative with equal probabilities.

2. THE MAIN THEOREM

We start with the definition of a knot diagram K as an oriented graph with crossing knot L . We draw it in the plane as a long knot diagram D in such a way that the strands intersecting at each crossing are pointing up (that's always possible because we can always rotate crossings as needed), and so that its beginning and end are at its two ends in the upward direction. We call such a diagram a *upright knot diagram*. An example of an upright knot diagram is shown on the right.

We then label each edge of the diagram with two labels: a *running index* k which runs from 1 to $n-1$, and a *“rotation number”* φ_k , the geometric rotation number of that edge¹. In

¹The signed number of times the tangent to the edge is horizontal and heading right, with loops counted with a sign and caps with -1 this would be defined at each node, all edges are headed up.

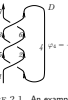


FIGURE 2.1. An example upright knot diagram.

In particular, the middle diagram which resembles the Greek letter Θ will have the invariant Θ .

Comment 3. The computation of G is bottleneck for the computation of Θ . It requires inverting a $(2n+1) \times (2n+1)$ matrix whose entries are (degree 1) Laurent polynomials in T . It's a daunting task but it takes polynomial time. Even a naive inversion using Gaussian elimination requires only n^3 operations in the ring $Q(T)$. If G can be computed in practice in $O(n^3)$ time, then Θ will be in $O(n^5)$.

The polynomials $F_1(c), F_2(c)$ and $F_3(c)$ are not unique, and we are not certain that we have the cleanest possible formula for them. They are ugly from a human perspective yet from a computational perspective, having 18 terms (as is the case for $F_1(c)$) isn't really a problem.

Computationally, the term $F_3(c)$ in (6) is the middle one, and even it takes merely $\approx n^2$ operations in the ring $Q(T_1, T_2)$ to evaluate.

3. IMPLEMENTATIONS AND EXAMPLES

3.1. Implementation. A concise yet reasonably efficient implementation is worth a thousand formulas. It completely removes antiquated, it tests the theories, and it allows for experiments. Our next task is to implement. The section that follows was generated by a Mathematica notebook that is available at [BV3, Tethra]. A second implementation of Θ , using Python and SageMath ([https://www.sagemath.org/]), is available at <https://www.rolandoval.com/~TheTheta/>.

We start by loading the package *KnotTheory*² — it is only needed because it has many specific knots pre-defined. In the Section and in the Θ and Θ' mean “human input” while Θ means “computer output”.

²Once<< KnotTheory`>> loading knotTheory` version of October 29, 2024, 10:29:52.1361. Head over at: <https://mathematica.stackexchange.com/wiki/KnotTheory>.

Next we quickly define the module *Rot*, used to compute rotations, and *PolyPlot*, used to plot polynomials as bar codes and as hexagonal QR codes. We also show one usage example for each.

3.2. Example. On to examples! Starting with the trefoil knot.

3.2.1. Expand. Θ is Expandable.

3.2.2. ImageCompose. Loading knotTheory` version of October 29, 2024, 10:29:52.1361.

We urge the reader to compare the above output with the knot diagram in Figure 2.1.

3.2.3. PolyPlot. Θ is PolyPlotable.

3.2.4. ImageSize. Θ is ImageSizeable.

3.2.5. Labeled. Θ is Labeledable.

3.2.6. Axes. Θ is Axesable.

3.2.7. PlotRange. Θ is PlotRangeable.

3.2.8. ImageCompose. Θ is ImageComposeable.

3.2.9. TubePlot. Θ is TubePlotable.

3.2.10. AxesLabel. Θ is AxesLabelable.

3.2.11. Image. Θ is Imageable.

3.2.12. PlotLabel. Θ is PlotLabelable.

3.2.13. PlotStyle. Θ is PlotStyleable.

3.2.14. PlotRangeClipping. Θ is PlotRangeClippingable.

3.2.15. PlotRangePadding. Θ is PlotRangePaddingable.

3.2.16. PlotRange. Θ is PlotRangeable.

3.2.17. PlotLabel. Θ is PlotLabelable.

3.2.18. PlotRangeClipping. Θ is PlotRangeClippingable.

3.2.19. PlotRangePadding. Θ is PlotRangePaddingable.

3.2.20. PlotRange. Θ is PlotRangeable.

3.2.21. PlotLabel. Θ is PlotLabelable.

3.2.22. PlotRangeClipping. Θ is PlotRangeClippingable.

3.2.23. PlotRangePadding. Θ is PlotRangePaddingable.

3.2.24. PlotRange. Θ is PlotRangeable.

3.2.25. PlotLabel. Θ is PlotLabelable.

3.2.26. PlotRangeClipping. Θ is PlotRangeClippingable.

3.2.27. PlotRangePadding. Θ is PlotRangePaddingable.

3.2.28. PlotRange. Θ is PlotRangeable.

3.2.29. PlotLabel. Θ is PlotLabelable.

3.2.30. PlotRangeClipping. Θ is PlotRangeClippingable.

3.2.31. PlotRangePadding. Θ is PlotRangePaddingable.

3.2.32. PlotRange. Θ is PlotRangeable.

3.2.33. PlotLabel. Θ is PlotLabelable.

3.2.34. PlotRangeClipping. Θ is PlotRangeClippingable.

3.2.35. PlotRangePadding. Θ is PlotRangePaddingable.

3.2.36. PlotRange. Θ is PlotRangeable.

3.2.37. PlotLabel. Θ is PlotLabelable.

3.2.38. PlotRangeClipping. Θ is PlotRangeClippingable.

3.2.39. PlotRangePadding. Θ is PlotRangePaddingable.

3.2.40. PlotRange. Θ is PlotRangeable.

3.2.41. PlotLabel. Θ is PlotLabelable.

3.2.42. PlotRangeClipping. Θ is PlotRangeClippingable.

3.2.43. PlotRangePadding. Θ is PlotRangePaddingable.

3.2.44. PlotRange. Θ is PlotRangeable.

3.2.45. PlotLabel. Θ is PlotLabelable.

3.2.46. PlotRangeClipping. Θ is PlotRangeClippingable.

3.2.47. PlotRangePadding. Θ is PlotRangePaddingable.

3.2.48. PlotRange. Θ is PlotRangeable.

3.2.49. PlotLabel. Θ is PlotLabelable.

3.2.50. PlotRangeClipping. Θ is PlotRangeClippingable.

3.2.51. PlotRangePadding. Θ is PlotRangePaddingable.

3.2.52. PlotRange. Θ is PlotRangeable.

3.2.53. PlotLabel. Θ is PlotLabelable.

3.2.54. PlotRangeClipping. Θ is PlotRangeClippingable.

3.2.55. PlotRangePadding. Θ is PlotRangePaddingable.

3.2.56. PlotRange. Θ is PlotRangeable.

3.2.57. PlotLabel. Θ is PlotLabelable.

3.2.58. PlotRangeClipping. Θ is PlotRangeClippingable.

3.2.59. PlotRangePadding. Θ is PlotRangePaddingable.

3.2.60. PlotRange. Θ is PlotRangeable.

3.2.61. PlotLabel. Θ is PlotLabelable.

3.2.62. PlotRangeClipping. Θ is PlotRangeClippingable.

3.2.63. PlotRangePadding. Θ is PlotRangePaddingable.

3.2.64. PlotRange. Θ is PlotRangeable.

3.2.65. PlotLabel. Θ is PlotLabelable.

3.2.66. PlotRangeClipping. Θ is PlotRangeClippingable.

3.2.67. PlotRangePadding. Θ is PlotRangePaddingable.

3.2.68. PlotRange. Θ is PlotRangeable.

3.2.69. PlotLabel. Θ is PlotLabelable.

3.2.70. PlotRangeClipping. Θ is PlotRangeClippingable.

3.2.71. PlotRangePadding. Θ is PlotRangePaddingable.

3.2.72. PlotRange. Θ is PlotRangeable.

3.2.73. PlotLabel. Θ is PlotLabelable.

3.2.74. PlotRangeClipping. Θ is PlotRangeClippingable.

3.2.75. PlotRangePadding. Θ is PlotRangePaddingable.

3.2.76. PlotRange. Θ is PlotRangeable.

3.2.77. PlotLabel. Θ is PlotLabelable.

3.2.78. PlotRangeClipping. Θ is PlotRangeClippingable.

3.2.79. PlotRangePadding. Θ is PlotRangePaddingable.

3.2.80. PlotRange. Θ is PlotRangeable.

3.2.81. PlotLabel. Θ is PlotLabelable.

3.2.82. PlotRangeClipping. Θ is PlotRangeClippingable.

3.2.83. PlotRangePadding. Θ is PlotRangePaddingable.

3.2.84. PlotRange. Θ is PlotRangeable.

3.2.85. PlotLabel. Θ is PlotLabelable.

3.2.86. PlotRangeClipping. Θ is PlotRangeClippingable.

3.2.87. PlotRangePadding. Θ is PlotRangePaddingable.

3.2.88. PlotRange. Θ is PlotRangeable.

3.2.89. PlotLabel. Θ is PlotLabelable.

3.2.90. PlotRangeClipping. Θ is PlotRangeClippingable.

3.2.91. PlotRangePadding. Θ is PlotRangePaddingable.

3.2.92. PlotRange. Θ is PlotRangeable.

3.2.93. PlotLabel. Θ is PlotLabelable.

3.2.94. PlotRangeClipping. Θ is PlotRangeClippingable.

3.2.95. PlotRangePadding. Θ is PlotRangePaddingable.

3.2.96. PlotRange. Θ is PlotRangeable.

3.2.97. PlotLabel. Θ is PlotLabelable.

3.2.98. PlotRangeClipping. Θ is PlotRangeClippingable.

3.2.99. PlotRangePadding. Θ is PlotRangePaddingable.

3.2.100. PlotRange. Θ is PlotRangeable.

3.2.101. PlotLabel. Θ is PlotLabelable.

3.2.102. PlotRangeClipping. Θ is PlotRangeClippingable.

3.2.103. PlotRangePadding. Θ is PlotRangePaddingable.

3.2.104. PlotRange. Θ is PlotRangeable.

3.2.105. PlotLabel. Θ is PlotLabelable.

3.2.106. PlotRangeClipping. Θ is PlotRangeClippingable.

3.2.107. PlotRangePadding. Θ is PlotRangePaddingable.

3.2.108. PlotRange. Θ is PlotRangeable.

3.2.109. PlotLabel. Θ is PlotLabelable.

3.2.110. PlotRangeClipping. Θ is PlotRangeClippingable.

3.2.111. PlotRangePadding. Θ is PlotRangePaddingable.

3.2.112. PlotRange. Θ is PlotRangeable.

3.2.113. PlotLabel. Θ is PlotLabelable.

3.2.114. PlotRangeClipping. Θ is PlotRangeClippingable.

3.2.115. PlotRangePadding. Θ is PlotRangePaddingable.

3.2.116. PlotRange. Θ is PlotRangeable.

3.2.117. PlotLabel. Θ is PlotLabelable.

3.2.118. PlotRangeClipping. Θ is PlotRangeClippingable.

3.2.119. PlotRangePadding. Θ is PlotRangePaddingable.

3.2.120. PlotRange. Θ is PlotRangeable.

3.2.121. PlotLabel. Θ is PlotLabelable.

3.2.122. PlotRangeClipping. Θ is PlotRangeClippingable.

3.2.123. PlotRangePadding. Θ is PlotRangePaddingable.

3.2.124. PlotRange. Θ is PlotRangeable.

3.2.125. PlotLabel. Θ is PlotLabelable.

3.2.126. PlotRangeClipping. Θ is PlotRangeClippingable.

3.2.127. PlotRangePadding. Θ is PlotRangePaddingable.

3.2.128. PlotRange. Θ is PlotRangeable.

3.2.129. PlotLabel. Θ is PlotLabelable.

3.2.130. PlotRangeClipping. Θ is PlotRangeClippingable.

3.2.131. PlotRangePadding. Θ is PlotRangePaddingable.

3.2.132. PlotRange. Θ is PlotRangeable.

3.2.133. PlotLabel. Θ is PlotLabelable.

3.2.134. PlotRangeClipping. Θ is PlotRangeClippingable.

3.2.135. PlotRangePadding. Θ is PlotRangePaddingable.

3.2.136. PlotRange. Θ is PlotRangeable.

3.2.137. PlotLabel. Θ is PlotLabelable.

3.2.138. PlotRangeClipping. Θ is PlotRangeClippingable.

3.2.139. PlotRangePadding. Θ is PlotRangePaddingable.

3.2.140. PlotRange. Θ is PlotRangeable.

3.2.141. PlotLabel. Θ is PlotLabelable.

3.2.142. PlotRangeClipping. Θ is PlotRangeClippingable.

3.2.143. PlotRangePadding. Θ is PlotRangePaddingable.

3.2.144. PlotRange. Θ is PlotRangeable.

3.2.145. PlotLabel. Θ is PlotLabelable.

3.2.146. PlotRangeClipping. Θ is PlotRangeClippingable.

3.2.147. PlotRangePadding. Θ is PlotRangePaddingable.

3.2.148. PlotRange. Θ is PlotRangeable.

3.2.149. PlotLabel. Θ is PlotLabelable.

3.2.150. PlotRangeClipping. Θ is PlotRangeClippingable.

3.2.151. PlotRangePadding. Θ is PlotRangePaddingable.

3.2.152. PlotRange. Θ is PlotRangeable.

3.2.153. PlotLabel. Θ is PlotLabelable.

3.2.154. PlotRangeClipping. Θ is PlotRangeClippingable.

3.2.155. PlotRangePadding. Θ is PlotRangePaddingable.

3.2.156. PlotRange. Θ is PlotRangeable.

